

Poly(propylene glycol)-*b*-Polylactide 블렌드 필름의 Stereocomplexation과 기계적 물성에 미치는 Poly(propylene glycol)의 블록 구조와 길이의 영향

Yodthong Baimark[†] and Yaowalak Srisuwan

Biodegradable Polymers Research Unit, Department of Chemistry and Center of Excellence for Innovation in Chemistry, Faculty of Science, Maharakham University

(2017년 9월 11일 접수, 2017년 11월 15일 수정, 2017년 11월 15일 채택)

Effects of Block Structure and Poly(propylene glycol) Block Length on Stereocomplexation and Mechanical Properties of Poly(propylene glycol)-*b*-Polylactide Blend Films

Yodthong Baimark[†] and Yaowalak Srisuwan

Biodegradable Polymers Research Unit, Department of Chemistry and Center of Excellence for Innovation in Chemistry, Faculty of Science, Maharakham University, Maharakham 44150, Thailand

(Received September 11, 2017; Revised November 15, 2017; Accepted November 15, 2017)

Abstract: Stereocomplex poly(lactide) (scPL) shows better mechanical properties than both poly(L-lactide) (PLL) and poly(D-lactide) (PDL). However, scPL is still brittle. In this work, di- and triblock copolymers of poly(propylene glycol) (PPG) and polylactide (PLL or PDL) were synthesized for the preparation of scPL films. The influences of the block structure, PPG block length and blend ratio on stereocomplexation, film morphology and mechanical properties of the scPL films were investigated. From DSC and WAXD results, the 50/50 wt% blend films exhibited the highest stereocomplexation. Phase separation between the scPL and PPG phases was not found from their SEM images. The tensile stress and elongation at break of the blend films increased with the stereocomplex crystallinities. The longer PPG blocks improved both the stereocomplexation and elongation at break of the blend films. In conclusion, the block structures and PPG block lengths influenced on both the stereocomplexation and mechanical properties of the scPL films.

Keywords: stereocomplex, polylactide, poly(propylene glycol), block copolymers, mechanical properties.

Introduction

Poly(L-lactic acid) (PLLA) or poly(L-lactide) (PLL) is an important bio-renewable and biodegradable polyester that has been widely studied for use in bioplastic applications. However, PLL products are limited for practical applications due to their high brittleness and low thermal resistance. Efficient plasticizers for PLL, such as poly(ethylene glycol) (PEG)¹⁻³ and poly(propylene glycol) (PPG),^{4,5} etc. have been reported to reduce the brittleness of the PLL. However, phase separation and migration behavior in these plasticizers have been reported, which reduced the plasticization effect.^{6,7} The attachment of these plasticizer molecules by block copolymerization

and reactive blending can improve the phase compatibility to reduce the migration effect of the plasticizers.^{8,9}

Polylactides (PL) has two enantiomers: poly(L-lactide) (PLL) and poly(D-lactide) (PDL). The PLL/PDL blending produced a stereocomplex PL (scPL), which exhibited better mechanical properties and heat resistance than both the PLL and PDL.¹⁰⁻¹⁴ The stronger interactions on the stereocomplex crystallites of the scPL induced a higher melting temperature ($T_m \approx 230$ °C) and faster crystallization rate than in either the original PLL or PDL ($T_m \approx 180$ °C).¹⁰ The faster crystallization of the scPL enhanced the good heat resistance. However, the scPL is still brittle due to its T_g being similar to those of PLL and PDL. Although stereocomplex formation of scPL has been extensively reported, there are only a limited number of works on the improvement of scPL flexibility by block copolymerization.

The PDL-PEG-PDL triblock copolymers have been synthesized and blended with PLL to form more flexible scPL

[†]To whom correspondence should be addressed.
yodthong.b@msu.ac.th, ORCID[®]0000-0001-8432-8721
©2018 The Polymer Society of Korea. All rights reserved.

films.^{8,15-18} The stereocomplexation of PLL-PEG-PLL/PDL-PEG-PDL blends has also been reported.¹⁹ Good phase compatibility between the PL and PEG phases was observed for these triblock copolymer blend films. The triblock copolymer blending showed synergistic effects of stereocomplexation between the two enantiomeric PLL and PDL chains, and plasticization of the PEG blocks. To the best of our knowledge, the influence of the PPG-PLL/PPG-PDL block copolymer blending on the stereocomplexation and mechanical properties of the scPL has not been reported so far. The PPG has also been shown to give efficient plasticization to improve the flexibility of the PLL^{4,5} and scPL.⁶ However, phase separation was observed for scPL/PPG blends with higher PPG molecular weight.⁶

In this paper, the stereocomplex blend films of PPG-PLL/PPG-PDL block copolymer blends prepared with different block structures (di- and triblock), PPG block lengths (2000 and 4000 g/mol) and blend ratios (75/25, 50/50 and 25/75 wt%) were prepared as scPL films by solution blending before film casting. The obtained results were also compared with the neat di- and triblock copolymer films (100/0 and 0/100 wt%).

Experimental

Materials. The L-lactide (LL) and D-lactide (DL) monomers were synthesized from L-lactic acid (88%, Purac, Thailand) and D-lactic acid (90%, Haihang Industry Co., Ltd., China), respectively. Both the LL and DL monomers were purified by repeated re-crystallization from ethyl acetate four times before drying in a vacuum oven at 55 °C for 48 h. Poly(propylene glycol) with molecular weights of 2000 (PPG2K) and 4000 (PPG4K) g/mol (Acros Organics) and a poly(propylene glycol) monobutyl ether with a molecular weight of 2500 (mPPG2.5K) g/mol (Acros Organics) were used as received. Stannous octoate (Sn(Oct)₂, 95% Sigma-Aldrich) was used without further purification. All solvents were analytical grade and used as received.

Synthesis of Block Copolymers. The diblock copolymers of mPPG-PLL and mPPG-PDL as well as triblock copolymers of PLL-PPG-PLL and PDL-PPG-PDL were synthesized by ring-opening polymerization in bulk of the LL and DL monomers under a nitrogen atmosphere at 165 °C for 4 h. The mPPG/Sn(Oct)₂ and PPG/Sn(Oct)₂ were used as the initiating systems for synthesizing the di- and triblock copolymers, respectively. The Sn(Oct)₂ concentration was kept constant at 0.01 mol%. The theoretical molecular weights of each PLL

and PDL block were 40000 g/mol. The block copolymers were purified by being dissolved in chloroform before being precipitated in cool *n*-hexane. They were then dried in a vacuum oven at room temperature for 48 h. According to this procedure, all the purified block copolymers were obtained with more than 95% yields.

Characterization of Block Copolymers. The chemical composition and number-average molecular weight (M_n) of the copolymers were determined by ¹H NMR spectrometry using a Bruker Advance DPX 400 ¹H NMR spectrometer at 25 °C. CDCl₃ was used as the solvent.

The M_n and polydispersity index (PDI) of the copolymers were measured by gel permeation chromatography (GPC) using a Waters e2695 separations module equipped with PLgel 10 μm mixed B 2 columns operating at 40 °C and employing a refractive index (RI) detector. Tetrahydrofuran was used as the solvent at a flow rate of 1.0 mL/min.

The specific optical rotation of the lactyl unit (half of lactide unit) of the copolymers ($[\alpha_{\text{lactyl}}]_{25}$) was investigated at 25 °C using a Bellingham and Stanley Polarimeter ADP220 at a wavelength of 589 nm with 1.0 dm sample tube length. Chloroform was used as the solvent at a concentration of approximately 1.0 g/dL. The $[\alpha_{\text{lactyl}}]_{25}$ was calculated by the following equation:

$$[\alpha_{\text{lactyl}}]_{25} = \alpha_{\text{lactide}} / (2 \cdot c) \quad (1)$$

where α_{lactide} was the optical rotation of the lactide unit (deg) and c was the sample concentration (g/cm³).

The thermal transition properties of the copolymers were determined by non-isothermal differential scanning calorimetry (DSC) using a Perkin-Elmer Pyris Diamond DSC. For DSC, samples of 3-5 mg in weight were heated at 10 °C/min over a temperature range of 0 to 250 °C (the 1st heating scan). The temperature was held at 250 °C for 3 min to erase the thermal history. Then, the samples were quenched to 0 °C according to the DSC instrument's own default cooling mode before heating from 0 to 250 °C (the 2nd heating scan).

Preparation of Blend Films. The mPPG2.5K-PLL and mPPG2.5K-PDL were dissolved separately. These copolymer solutions were then admixed under vigorous stirring for 30 min. The final concentration of the blend solution was 1.0 g/dL in chloroform. The blend solutions were cast onto glass petri-dishes, followed by solvent evaporation at room temperature for 24 h before drying in a vacuum oven for 48 h to evaporate any residue solvent. The blend films with the

mPPG2.5K-PLL/mPPG2.5K-PDL blend ratios of 100/0, 75/25, 50/50, 25/75 and 0/100 wt% were prepared. The PLL-PPG2K-PLL/PDL-PPG2K-PDL and PLL-PPG4K-PLL/PDL-PPG4K-PDL blend films with various blend ratios were prepared by the same method.

Characterization of Blend Films. The thermal transition properties of the blend films were determined by non-isothermal differential scanning calorimetry (DSC) from the 2nd heating scan. The degrees of homo-crystallinity (X_{hc}) and stereocomplex crystallinity (X_{sc}) of the blend films were determined from the enthalpies of melting of the homo-crystallites (ΔH_{hc}) and stereocomplex crystallites (ΔH_{sc}) using eq. (2) and (3), respectively.

$$X_{hc}(\%) = [\Delta H_{hc}/(w_{PL} \times 93.7 \text{ J/g})] \times 100 \quad (2)$$

$$X_{sc}(\%) = [\Delta H_{sc}/(w_{PL} \times 142 \text{ J/g})] \times 100 \quad (3)$$

where the enthalpies of melting for 100% crystallinity of the homo- and stereocomplex crystallites were 93.7 and 142 J/g, respectively.⁶ The w_{PL} was the weight fraction of the polylactide (PL) including PLL and PDL in the blend films that were obtained from ¹H NMR. Relative fractions of stereocomplex crystallites (f_{sc}) was determined by eq. (4).¹⁹

$$f_{sc}(\%) = [X_{sc}/(X_{hc} + X_{sc})] \times 100 \quad (4)$$

The crystalline structures of the blend films were investigated by wide-angle X-ray diffractometry (WAXD) using a Bruker D8 Advance wide-angle X-ray diffractometer at 25 °C. CuK α radiation at 40 kV and 40 mA was chosen. For WAXD, the scanning angle range of $2\theta = 5\text{--}30^\circ$ at a scan speed of 3°/min was used.

The phase morphologies of the film cross-sections were determined using a JEOL JSM-6460LV scanning electron microscopy (SEM). The samples were sputter-coated with gold to enhance the surface conductivity before scanning.

The mechanical properties, including stress at break, elongation at break and initial Young's modulus, of the blend films were measured at 25 °C and 65% relative humidity using a Lloyds LRX+ universal mechanical testing machine. The film samples (10×100 mm) were tested with a gauge length of 25 mm and a crosshead speed of 10 mm/min. The mechanical properties were determined from the average of five measurements for each sample.

Results and Discussion

Characterization of Block Copolymers. Information about the mPPG-PL diblock and PL-PPG-PL triblock copolymers are reported in Table 1. The mPPG and PPG containing one and two hydroxyl end-groups were used to synthesize the copolymers with di- and triblock structures, respectively. The molecular weights of the mPPG and PPG blocks were noted. Meanwhile, the feed molecular weights of the PLL and PDL blocks were approximate 40000 g/mol.

The ¹H NMR spectra were used to identify the chemical structures of the block copolymers, and examples are shown in Figure 1 for the mPPG-PDL and PDL-PPG-PDL block copolymers. The propylene oxide (PO) units of the mPPG and PPG blocks showed peaks of methyl protons (-CH₃, a), methine protons (-CH, b) and methylene protons (-CH₂, c) at $\delta = 1.1$, 3.5 and 3.4 ppm, respectively.²⁰ The DL units of the PDL blocks showed peaks of methyl protons (-CH₃, d) at $\delta = 1.6$ ppm and methine protons (-CH, e) at $\delta = 5.2$ ppm. The ¹H

Table 1. Information, Chemical Composition and Molecular Weight of Block Copolymers

Block copolymer	M.W. of PPG block	Feed PO/L ratio ^a (mol%)	Final PO/L ratio ^b (mol%)	M_n^b (g/mol)	M_n^c (g/mol)	PDI ^c
Diblock copolymer						
mPPG2.5K-PLL	2500	13/87	12/88	47000	37400	1.3
mPPG2.5K-PDL	2500	13/87	12/88	47000	37700	1.7
Triblock copolymer						
PLL-PPG2K-PLL	2000	6/94	7/93	67000	60300	1.6
PDL-PPG2K-PDL	2000	6/94	7/93	67000	85800	1.3
PLL-PPG4K-PLL	4000	11/89	11/89	83300	56600	1.5
PDL-PPG4K-PDL	4000	11/89	11/89	83300	61900	1.4

^aCalculated from weights of feed PPG and feed lactide. ^bCalculated from ¹H NMR. ^cDetermined from GPC.

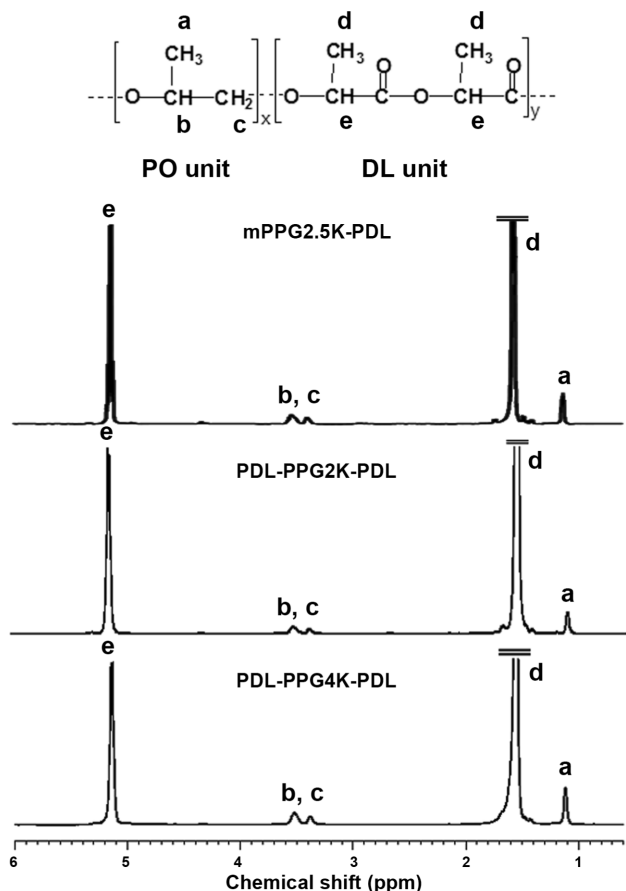


Figure 1. ^1H NMR spectra of mPPG-PDL diblock and PDL-PPG-PDL triblock copolymers (peak assignments as shown).

NMR spectra of the mPPG-PLL and PLL-PPG-PLL illustrated similar results to the mPPG-PDL and PDL-PPG-PDL, respectively. The chemical compositions of the block copolymers were measured from the ^1H NMR spectra. The PO/LL and PO/DL mole ratios of the block copolymers were determined by ratioing the integral peak areas corresponding to the PO methyl protons (peak a) and lactide methine protons (peak e). The final PO/LL and PO/DL ratios calculated from the ^1H NMR are reported in Table 1. As would be expected, the copolymer compositions from the ^1H NMR are very similar to the feed ratios. Therefore, the synthesis reactions were taken to be a quantitative conversion.

The M_n s of the block copolymers calculated from the PO/LL (or PO/DL) ratios and PPG molecular weight are also summarized in Table 1. Each block copolymer showed only a single GPC curve with a unimodal molecular weight distribution indicating successful block copolymerization, with examples shown in Figure 2 for mPPG-PDL and PDL-PPG-PDL. Their M_n and PDI values obtained from the GPC are also reported in

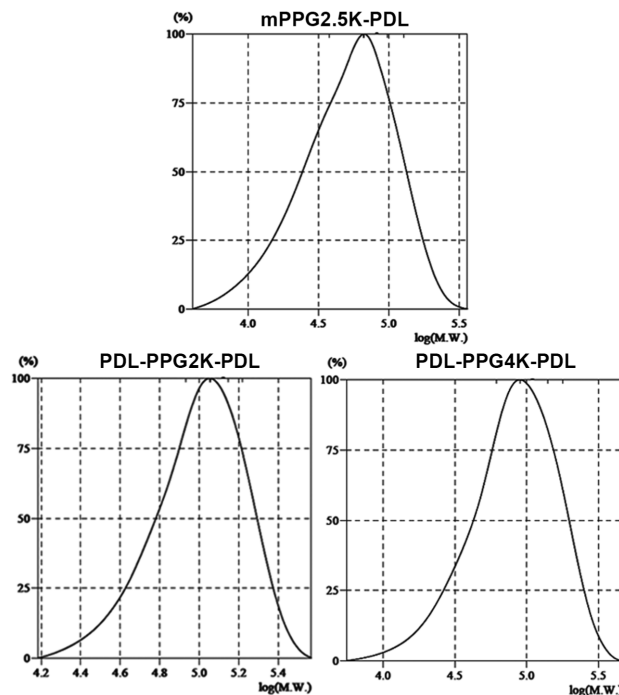


Figure 2. GPC curves of mPPG-PDL diblock and PDL-PPG-PDL triblock copolymers.

Table 1. The M_n s of the PL-PPG2K-PL triblock copolymers were higher than the mPPG2.5K-PL diblock copolymers. All the PDI values were similarly narrow in the range 1.3-1.7.

The ^1H NMR and GPC results suggested that PPG-PLL and PPG-PDL block copolymers with different block structures (di- and triblock) and PPG block lengths (2K and 4K g/mol) were successfully synthesized to determine the influences of the block structure and PPG block length on the stereocomplexation and mechanical properties.

The $[\alpha_{\text{lactyl}}]_{25}$ of the copolymers are reported in Table 2, and these suggest that the block copolymers of PLL and PDL contained predominantly the L-form and D-form, respectively. It has been reported that the $[\alpha_{\text{lactyl}}]_{25}$ values were -156 and $+156$ $\text{deg}\cdot\text{cm}^3/\text{dm}\cdot\text{g}$ for the PLL and PDL, respectively.²¹ The $[\alpha_{\text{lactyl}}]_{25}$ values of these block copolymers were lower due to the PPG content. The $[\alpha_{\text{lactyl}}]_{25}$ values of the PL-PPG2K-PL were larger than the mPPG2.5K-PL. This was due to another PL end-block being attached for the PL-PPG2K-PL. The $[\alpha_{\text{lactyl}}]_{25}$ values of the PL-PPG-PL decreased slightly as the PPG block lengths increased from 2000 to 4000 g/mol.

The thermal transition properties of the block copolymers from the DSC curves (not shown) are also summarized in Table 2. Their T_m s were similar in the range 170 - 174 $^\circ\text{C}$. The ΔH_m s and T_g s of the PL blocks of PL-PPG2K-PL were slightly

Table 2. Specific Optical Rotations and Thermal Transition Properties of Block Copolymers

Block copolymer	$[\alpha_{\text{actyl}}]_{25}$ (deg.cm ³ /dm.g) ^a	T_m (°C) ^b	ΔH_m (J/g) ^b	T_g (°C) ^c
Diblock copolymer				
mPPG2.5K-PLL	-137.8	174	45.0	54
mPPG2.5K-PDL	+134.9	173	46.2	53
Triblock copolymer				
PLL-PPG2K-PLL	-141.9	174	49.6	56
PDL-PPG2K-PDL	+141.6	174	50.8	56
PLL-PPG4K-PLL	-138.6	170	46.6	50
PDL-PPG4K-PDL	+138.8	172	48.9	51

^aDetermined from polarimetry. ^bObtained from 1st heating scan DSC curves. ^cObtained from 2nd heating scan DSC curves.

higher than the mPPG2.5K-PL. This was due to the two PL end-blocks of PL-PPG2K-PL inducing larger PL crystallites. However, the T_g s of the PL end-blocks of PL-PPG-PL slightly decreased when the PPG middle-block length increased from 2000 to 4000 g/mol.

Stereocomplexation of Blend Films. The expanded 2nd heating scan DSC thermograms were used to investigate the stereocomplex formation of the mPPG2.5K-PLL/mPPG2.5K-PDL, PLL-PPG2K-PLL/PDL-PPG2K-PDL and PLL-PPG4K-PLL/PDL-PPG4K-PDL blend films, as illustrated in Figure 3. All the neat block copolymer films showed only T_m values of homo-crystallites ($T_{m,hc}$) in the range 155-175 °C. All the blend films exhibited both T_m of homo- ($T_{m,hc}$) and stereocomplex crystallites ($T_{m,sc}$). The $T_{m,sc}$ peaks of the blend films were broad in range 200-250 °C. The DSC results of the mPPG2.5K-PLL/mPPG2.5K-PDL, PLL-PPG2K-PLL/PDL-PPG2K-PDL and PLL-PPG4K-PLL/PDL-PPG4K-PDL blend films are summarized in Tables 3-5, respectively. It was found that the X_{hc} of the blend films decreased and the X_{sc} increased when the blend ratios were adjusted to 50/50 wt%. All the 50/50 blend films showed the highest f_{sc} values. This due to they were equimolar ratio.

The f_{sc} of the mPPG2.5K-PL and PL-PPG4K-PL blend films in Tables 3 and 5, respectively, were higher than the PL-PPG2K-PL blend films in Table 4 for the same blend ratio. This may be explained by the triblock structure of the PL-PPG2K-PL blend films reducing the chain mobility for stereocomplexation when compared to the mPPG2.5K-PL blend films. In addition, the longer PPG block of the PL-PPG4K-PL blend films may enhance the chain mobility to improve the stereocomplexation. In addition, the f_{sc} of the 50/50 PL-PPG2K-PL and PL-PPG4K-PL blend films in this work were very high compared to the PL-PEG-PL blend films with similar PEG

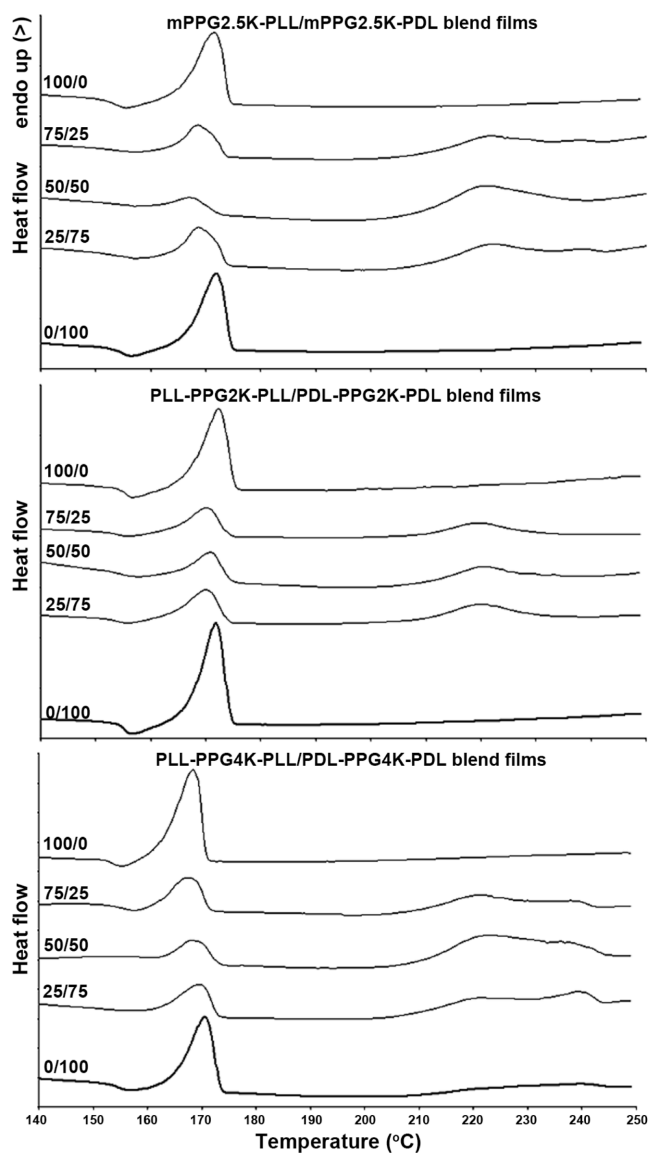


Figure 3. 2nd heating scan DSC curves of diblock and triblock copolymer blend films with different blend ratios.

Table 3. Thermal Transition Properties of mPPG2.5K-PLL/mPPG2.5K-PDL Blend Films from 2nd Heating Scan DSC Curves

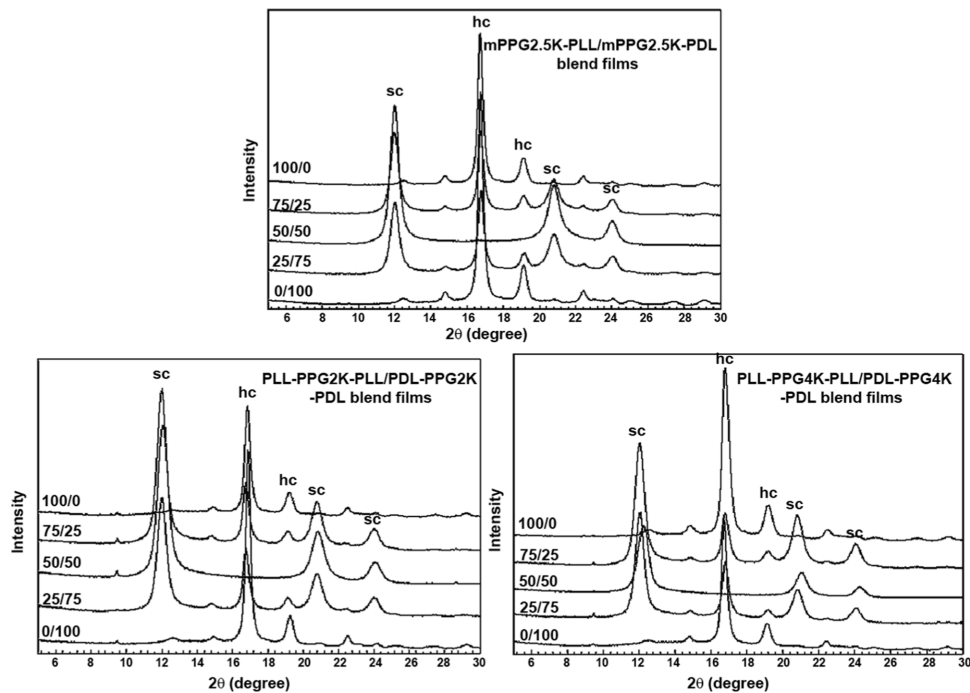
mPPG2.5K-PLL/mPPG2.5K-PDL blend ratio (wt%)	T_g (°C)	T_c (°C)	ΔH_c (J/g)	$T_{m,hc}$ (°C)	ΔH_{hc} (J/g)	X_{hc} (%)	$T_{m,sc}$ (°C)	ΔH_{sc} (J/g)	X_{sc} (%)	f_{sc} (%)
100/0	53	90	-25.7	172	51.8	55.3	-	-	-	0
75/25	52	83	-8.3	169	22.2	23.7	222	27.1	19.1	44.6
50/50	53	80	-4.5	167	11.3	12.1	221	46.3	32.6	72.9
25/75	53	82	-10.3	169	25.4	27.1	222	31.2	22.0	44.8
0/100	53	93	-26.8	172	51.3	54.8	-	-	-	0

Table 4. Thermal Transition Properties of PLL-PPG2K-PLL/PDL-PPG2K-PDL Blend Films from 2nd Heating Scan DSC Curves

PLL-PPG2K-PLL/PDL-PPG2K-PDL blend ratio (wt%)	T_g (°C)	T_c (°C)	ΔH_c (J/g)	$T_{m,hc}$ (°C)	ΔH_{hc} (J/g)	X_{hc} (%)	$T_{m,sc}$ (°C)	ΔH_{sc} (J/g)	X_{sc} (%)	f_{sc} (%)
100/0	56	97	-28.9	172	57.2	61.0	-	-	-	0
75/25	56	98	-20.2	171	21.7	23.2	219	21.6	15.2	39.6
50/50	56	99	-22.6	171	21.8	23.3	220	25.6	18.0	43.6
25/75	55	97	-25.2	170	24.6	26.2	220	25.7	18.1	40.8
0/100	56	97	-34.6	172	60.7	64.8	-	-	-	0

Table 5. Thermal Transition Properties of PLL-PPG4K-PLL/PDL-PPG4K-PDL Blend Films from 2nd Heating Scan DSC Curves

PLL-PPG4K-PLL/PDL-PPG4K-PDL blend ratio (wt%)	T_g (°C)	T_c (°C)	ΔH_c (J/g)	$T_{m,hc}$ (°C)	ΔH_{hc} (J/g)	X_{hc} (%)	$T_{m,sc}$ (°C)	ΔH_{sc} (J/g)	X_{sc} (%)	f_{sc} (%)
100/0	51	89	-26.5	168	49.7	53.0	-	-	-	0
75/25	51	84	-11.0	168	21.2	22.6	221	32.4	22.8	50.2
50/50	51	78	-5.6	168	13.8	14.7	222	60.0	42.2	74.2
25/75	52	83	-11.1	169	22.6	24.1	221	34.1	24.0	49.9
0/100	52	88	-24.5	170	43.1	46.0	-	-	-	0

**Figure 4.** WAXD patterns of diblock and triblock copolymer blend films with different blend ratios.

middle and PL end block lengths.¹⁹ This may be due to the non-crystallizability of PPG chains enhanced the stereocomplex crystallization of the PL blocks.

The T_g values of the blend films were similar to their neat block copolymers (see Table 2), which indicates that the stereocomplexation did not affect the glassy-rubbery transition of the blend films. The T_g values of the mPPG2.5K-PLL/mPPG2.5K-PDL, PLL-PPG2K-PLL/PDL-PPG2K-PDL and PLL-PPG4K-PLL/PDL-PPG4K-PDL blend films were in the ranges 52-53, 55-56 and 51-52 °C, respectively. The crystallization temperatures (T_c) and heat of crystallization (ΔH_c) of the blend films decreased steadily when the blend ratios were adjusted to 50/50 wt%, except the PLL-PPG2K-PLL/PDL-PPG2K-PDL blend films. The results indicate that the good stereocomplexation of 50/50 blend films enhanced crystallization. The triblock structure and shorter PPG blocks of PL-PPG2K-PL blend films reduced chain mobility for crystallization.

Figure 4 shows the WAXD patterns of the neat block copolymer and blend films to determine the homo- (hc) and stereocomplex (sc) crystalline structures. All the neat triblock copolymer films presented only diffraction peaks of the hc crystallites at 2θ of 17° and 19°. Meanwhile, all the 50/50 wt% blend films exhibited only diffraction peaks of the sc crys-

tallites at 2θ of 12°, 21° and 24°.²² This suggested that the blend films with the 50/50 wt% ratio had complete stereocomplexation. The WAXD patterns of the 75/25 and 25/75 wt% blend films exhibited the diffraction peaks of both the hc and sc crystallites. These blend films contained predominantly the sc crystallites.

Phase Morphology of Blend Films. The phase morphologies of the blend films were observed from the SEM images of their film cross-sections as shown in Figure 5 for the 50/50 wt% blend films. They were smooth without internal voids suggested that phase separation between the PL and the PPG blocks did not occur. The different block structures and PPG block lengths of the blend films did not induce phase separation. The neat block copolymer as well as the 75/25 and 25/75 wt% blend films also exhibited smooth surfaces. The scPL/PPG blend films showed phase separation between the scPL and PPG phases. The internal voids were detected on the film cross-sections of scPL/PPG blends, as shown in our previous work.⁶ This indicates that the block copolymer structures enhanced the phase compatibility between the PL and PPG components for all the neat block copolymer and blend films.

Tensile Properties of Blend Films. Figure 6 shows the tensile curves of the neat block copolymer and blend films. All the blend films exhibited higher stress and elongation at break

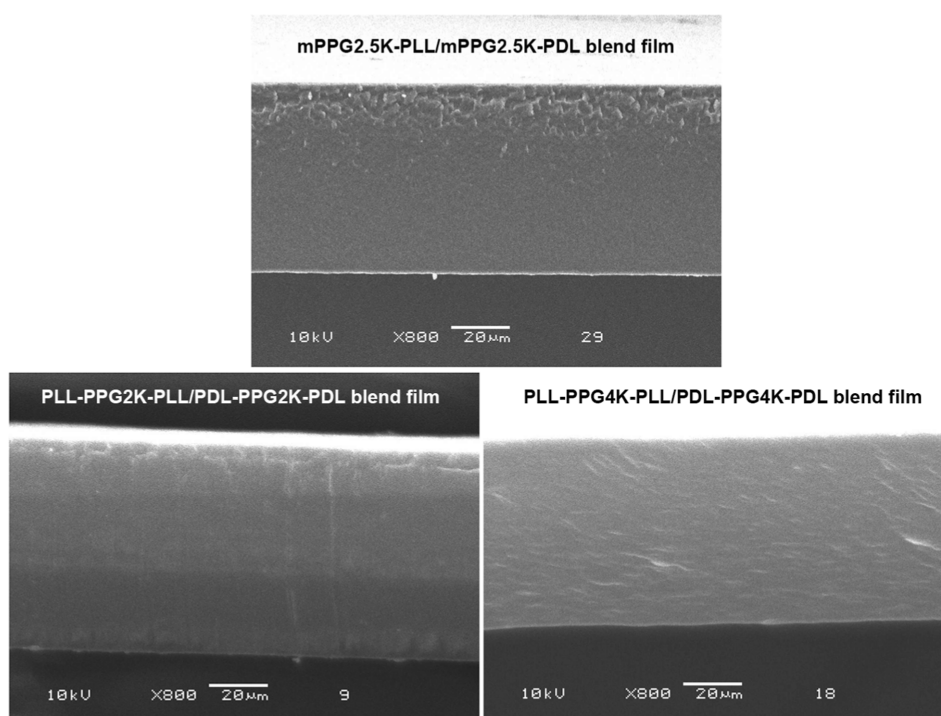


Figure 5. SEM images of cross-sections of 50/50 wt% blend films (all scale bars = 20 µm).

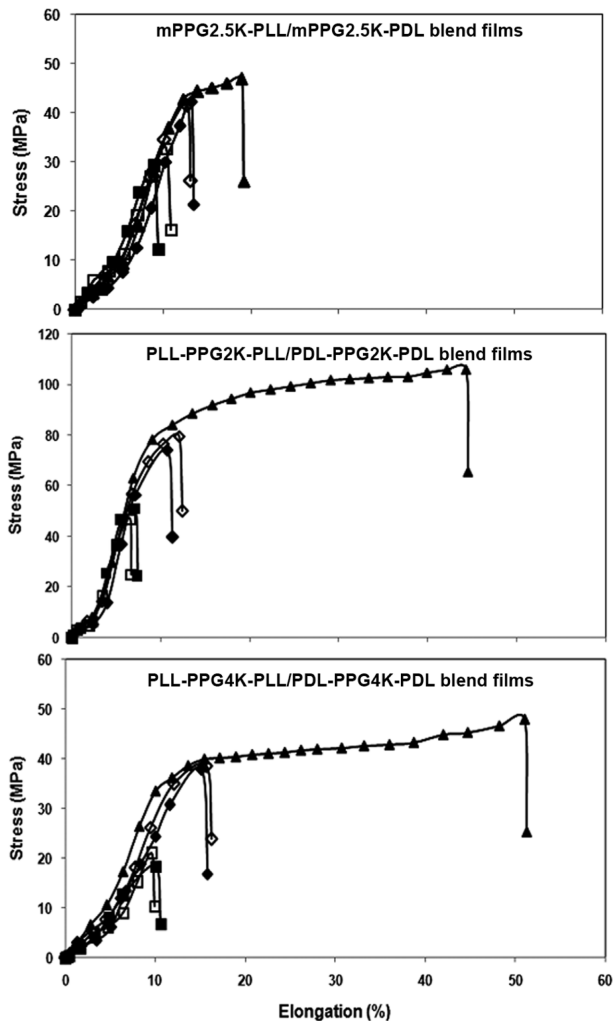


Figure 6. Tensile curves of block copolymer blend films prepared with blend ratios of (□) 100/0, (◇) 75/25, (▲) 50/50, (◆) 25/75 and (■) 0/100 wt%.

than the neat block copolymer films. This was due to the sc crystallites having stronger interactions than the hc crystallites.¹⁴ The 50/50 wt% blend films of each blend film series had the highest stress and elongation at break because the 50/50 wt% blend films were complete stereocomplexation from the WAXD results. The sc crystallites enhanced mechanical properties better than the hc crystallites.¹⁰ Meanwhile the 75/25 and 25/75 wt% blend films consisted both the hc and sc crystallites.

Table 6 summarizes the average values of the tensile properties, including Young's modulus, stress at break and elongation at break, of the neat block copolymer and blend films. In each blend film series, the Young's modulus did not change significantly with the blend ratio. Thus, the stereocomplexation

Table 6. Tensile Properties of Block Copolymer Blend Films

Block copolymer blend ratio (wt%)	Initial Young's modulus (MPa)	Stress at break (MPa)	Elongation at break (%)
mPPG2.5K-PLL/mPPG2.5K-PDL			
100/0	539±56	32.9±7.8	9.4±1.3
75/25	693±69	47.0±0.4	13.0±0.6
50/50	574±118	47.4±4.3	20.7±1.6
25/75	565±80	43.3±2.5	14.9±1.9
0/100	445±103	21.6±6.6	8.9±0.6
PLL-PPG2K-PLL/PDL-PPG2K-PDL			
100/0	1492±185	55.4±6.2	8.1±1.2
75/25	1471±102	78.4±5.9	14.7±2.6
50/50	1513±127	98.7±11.2	51.3±10.2
25/75	1532±215	81.6±7.3	12.9±3.7
0/100	1582±185	62.1±8.8	7.8±2.5
PLL-PPG4K-PLL/PDL-PPG4K-PDL			
100/0	1090±112	18.7±5.1	12.4±2.3
75/25	1112±98	41.2±6.4	17.2±3.6
50/50	1134±121	50.4±12.7	59.2±11.5
25/75	978±137	37.8±7.1	16.4±4.1
0/100	1159±166	17.5±4.6	11.8±2.7

did not affect the Young's modulus of the block copolymer blend films. The Young's modulus values of the PLL-PPG2K-PLL/PDL-PPG2K-PDL triblock copolymer blend films (1471-1582 MPa) were higher than the mPPG2.5K-PLL/mPPG2.5K-PDL diblock copolymer blend films (445-693 MPa). The Young's modulus of the film samples decreased as the PPG block length increased from 2000 to 4000 g/mol.

Both the stress and elongation at break of each blend film series increased when the blend ratio was changed to 50/50 wt%. The stress and elongation at break of the 50/50 wt% mPPG2.5K-PLL/mPPG2.5K-PDL blend film was lower than the 50/50 wt% PLL-PPG2K-PLL/PDL-PPG2K-PDL blend film. The triblock structure of PL-PPG-PL copolymers improved the mechanical properties of blend films. However, the stress at break of the 50/50 wt% triblock copolymer blend films decreased and the elongation at break increased when the PPG middle-block lengths increased from 2000 to 4000 g/mol. This suggests that the longer PPG block induced a better plasticization effect corresponding to the lower T_g of the PLL-PPG4K-PLL/PDL-PPG4K-PDL blends (see Tables 4 and 5).

The elongations at break of the 50/50 wt% block copolymer blend films in this work were higher than the 50/50 wt% PLL/PDL blend films (~9%).⁶ Therefore, the PPG blocks on the di-

and triblock copolymers in this work improved the flexibility of the scPL films similar to the PEG blocks of the stereocomplex PLL-PEG-PLL/PDL-PEG-PDL blend films.¹⁹ The flexible PPG blocks enhanced the plasticization effect under mechanical deformation. The results suggested that the mechanical properties of the blend films depended on the stereocomplexation, block structure and PPG block length.

Conclusions

The stereocomplex block copolymer films of the mPPG-PLL/mPPG-PDL and PLL-PPG-PLL/PDL-PPG-PDL blends were prepared by solution blending. The DSC results indicated that the 50/50 wt% blend films of each blend film series had the highest f_{sc} values. The WAXD results showed that the 50/50 wt% blend films had complete stereocomplexation. The 75/25 and 25/75 wt% blend films had stereocomplex crystallites as the major crystallites. The greater chain mobility of the diblock structure and longer PPG block enhanced the stereocomplexation. The phase separation of all the blend films could not be observed from their SEM images. All the blend films exhibited higher stress and elongation at break than those of the neat block copolymer films. The 50/50 wt% blend films showed the highest mechanical properties. The triblock structure and longer PPG block of the blend films improved the elongation at break. These block copolymer blend films were more flexible than the scPL film. In conclusion, the stereocomplexation and mechanical properties of the blend films can be tailored by adjusting the blend ratio, block structure and PPG block length of the block copolymers.

Acknowledgments: The authors gratefully acknowledge the Division of Research Facilitation and Dissemination, Mahasarakham University (2016) for its financial support. The Center of Excellence for Innovation in Chemistry (PERCH-CIC), Office of the Higher Education Commission, Ministry of Education (OHEC), Thailand is also acknowledged. The authors are very grateful to Dr. Jolyon Dodgson, Department of Biology, Faculty of Science, Mahasarakham University for his improvement of the English language in this manuscript.

References

1. I. Pillin, N. Montrelay, and Y. Grohens, *Polymer*, **47**, 4676 (2006).
2. Y. Hu, Y. S. Hu, V. Topolkarayev, A. Hiltner, and E. Baer, *Polymer*, **44**, 5711 (2003).
3. S. Z. Rogovina, K. V. Aleksanyan, A. A. Kosarev, N. E. Ivanushkina, E. V. Prut, and A. A. Berlin, *Polym. Sci. Series B*, **58**, 38 (2016).
4. Z. Kulinski, E. Piorkowska, K. Gadzinowska, and M. Stasiak, *Biomacromolecules*, **7**, 2128 (2006).
5. E. Piorkowska, Z. Kulinski, A. Galeski, and R. Masirek, *Polymer*, **47**, 7178 (2006).
6. K. Pakkethati and Y. Baimark, *Polym. Sci. Series A*, **59**, 124 (2017).
7. M. Baiardo, G. Frisoni, M. Scandola, M. Rimelen, D. Lips, K. Ruffieux, and E. Wintermantel, *J. Appl. Polym. Sci.*, **90**, 1731 (2003).
8. S. Tacha, T. Saelee, W. Khotasen, W. Punyodom, R. Molloy, P. Worajittiphon, P. Meepowpan, and K. Manokruang, *Eur. Polym. J.*, **69**, 308 (2015).
9. F. Hassouna, J. M. Raquez, F. Addiego, P. Dubois, V. Toniazzo, and D. Ruch, *Eur. Polym. J.*, **47**, 2134 (2011).
10. H. Tsuji, *Macromol. Biosci.*, **5**, 569 (2005).
11. H. Tsuji, *Biomaterials*, **24**, 537 (2003).
12. S. Li and M. Vert, *Macromolecules*, **36**, 8008 (2003).
13. K. Fukushima, Y. H. Chang, and Y. Kimura, *Macromol. Biosci.*, **7**, 829 (2007).
14. J. H. Kim, J. Jegal, B. K. Song, and C. H. Chin, *Polym. Korea*, **35**, 52 (2011).
15. Y. Liu, J. Shao, J. Sun, X. Bian, L. Feng, S. Xiang, B. Sun, Z. Chen, G. Li, and X. Chen, *Polym. Degrad. Stab.*, **101**, 10 (2014).
16. Y. Song, D. Wang, N. Jiang, and Z. Gan, *ACS Sustain. Chem. Eng.*, **3**, 1492 (2015).
17. Z. Jing, X. Shi, G. Zhang, and R. Lei, *Polym. Int.*, **64**, 1399 (2015).
18. Z. Jing, X. Shi, and G. Zhang, *Polymers*, **9**, 107 (2017).
19. L. Han, C. Yu, J. Zhou, G. Shan, Y. Bao, X. Yun, T. Dong, and P. Pan, *Polymer*, **103**, 376 (2016).
20. S. M. Ho and A. M. Young, *Eur. Polym. J.*, **42**, 1775 (2006).
21. H. Tsuji and Y. Ikada, *Macromolecules*, **25**, 5719 (1992).
22. G. Bibi, Y. Jung, J. C. Lim, and S. H. Kim, *Polym. Korea*, **39**, 453 (2015).